Heliyon 9 (2023) e15423

Contents lists available at ScienceDirect

Heliyon

journal homepage: www.cell.com/heliyon

Research article

Reduced pain sensitivity of episodic pain syndrome model mice carrying a Nav1.9 mutation by ANP-230, a novel sodium channel blocker

Hiroko Okuda [a,e,*], Sumiko Inoue [a], Yoshihiro Oyamada [a,b], Akio Koizumi [a,c,**], Shohab Youssefian [a,d]

[a] Department of Pain Pharmacogenetics, Graduate School of Medicine, Kyoto University, Kyoto, 606-8501, Japan
[b] AlphaNavi Pharma Inc., Osaka, 564-0053, Japan
[c] Institute of Public Health and Welfare Research, Kyoto, 616-8141, Japan
[d] Laboratory of Molecular Biosciences, Graduate School of Medicine, Kyoto University, Kyoto, 606-8501, Japan
[e] Department of Molecular Cell Physiology, Kyoto Prefectural University of Medicine, 465 Kajiicho Kamigyo-ward, Kyoto, 602-8566, Japan

ARTICLE INFO

Keywords:
Episodic pain syndrome
Pain model mice
Sodium channel blocker
Nav1.9 voltage-gated sodium channel
Behavioral experiments
Electrophysiology
Pharmacology
Non-opioid analgesics

ABSTRACT

The sodium channel Nav1.9 is expressed in the sensory neurons of small diameter dorsal root ganglia that transmit pain signals, and gain-of-function Nav1.9 mutations have been associated with both painful and painless disorders. We initially determined that some Nav1.9 mutations are responsible for familial episodic pain syndrome observed in the Japanese population. We therefore generated model mice harboring one of the more painful Japanese mutations, R222S, and determined that dorsal root ganglia hyperexcitability was the cause of the associated pain.

ANP-230 is a novel non-opioid drug with strong inhibitory effects on Nav1.7, 1.8 and 1.9, and is currently under clinical trials for patients suffering from familial episodic pain syndrome. However, little is known about its mechanism of action and effects on pain sensitivity.

In this study, we therefore investigated the inhibitory effects of ANP-230 on the hypersensitivity of Nav1.9 p.R222S mutant model mouse to pain. In behavioral tests, ANP-230 reduced the pain response of the mice, particularly to heat or mechanical stimuli, in a concentration- and time-dependent manner. Furthermore, ANP-230 suppressed the repetitive firing of dorsal root ganglion neurons of these mutant mice. Our results clearly demonstrate that ANP-230 is an effective analgesic for familial episodic pain syndrome resulting from DRG neuron hyperexcitability, and that such analgesic effects are likely to be of clinical significance.

1. Introduction

Voltage-gated sodium (Nav) channels consist of nine pore-forming alpha subunits, encoded by the *SCN1A-SCN11A* genes, coupled to beta subunits that function as modulators of the channel properties. Different alpha subunits have distinct electrophysiological properties, sensed by the voltage sensor in segment 4 (S4), thereby giving rise to nine Nav channel subtypes (Nav1.1–Nav1.9) with

Abbreviations: FEP, familial episodic pain.

* Corresponding author.
** Corresponding author. Department of Pain Pharmacogenetics, Graduate School of Medicine, Kyoto University, Kyoto, 606-8501, Japan.
E-mail addresses: okuda-h@kyoto.kpu-m.ac.jp (H. Okuda), koizumi@kyoto-hokenkai.or.jp (A. Koizumi).

https://doi.org/10.1016/j.heliyon.2023.e15423
Received 15 June 2022; Received in revised form 24 March 2023; Accepted 6 April 2023
Available online 14 April 2023

different voltage-dependent properties and kinetics [1]. These Nav channels are typed according to their pharmacological responses to tetrodotoxin (TTX) that binds to the Nav channels in nerve cell membranes and inhibits the firing of action potentials (APs) in the neurons, and include sensitive channels (TTXs), comprised of Nav1.1–1.4, Nav1.6 and Nav1.7, as well as resistant channels (TTXr), comprised of Nav1.5, Nav1.8, and Nav1.9 [2]. Nav channels also display tissue-specific expression, with Nav1.1 and Nav1.6 being predominantly expressed in the central nervous system (CNS), and Nav1.7, Nav1.8, and Nav1.9 in the peripheral nervous system (PNS) neurons. Nav1.9 has been found in all neuronal compartments in primary afferents that transduce mechanical, thermal and chemical signals to the CNS, but it is mainly found in unmyelinated C afferents, the majority of which belong to nociceptive neurons involved in the perception of pain [2].

Nociception conveys information about noxious stimuli from the PNS to the CNS via the dorsal root ganglion (DRG) that are located in the cell bodies of sensory neurons. The response of nociceptors to stimuli is encoded by the APs derived from Nav1.7–1.9. Here, Nav1.7 generates a transient Na^+ current, which has a slow rate of inactivation near the resting membrane potential (RMP) that allows the channel to generate persistent currents [2,3]; Nav1.8 has a depolarized activation voltage compared with Nav1.7 and Nav1.9 [1]; and Nav1.9 activates over a negative range of membrane potentials close to the RMP and generates a persistent inward current at a subthreshold voltage [4]. Therefore, activities of the three voltage gated sodium channels, i.e. Nav1.7, Nav1.8 and Nav1.9, contribute to pain signaling through AP generation at the PNS [1,4,5]. Mutations in Nav1.9 have been particularly associated with painful neuropathies, including familial episodic limb pain [6–9], congenital insensitivity to pain [10–13], and small fiber neuropathy [14–16], which are induced by the hypersensitivity of DRG neurons through repetitive AP firing [4,8,17].

From a nationwide survey in Japan, we previously found that early-onset familial episodic pain (FEP) syndrome can be caused by novel Nav1.9 mutations [8,18]. We were able to reproduce the pathogenic behavior of FEP and the hypersensitivity of the DRG neurons in a knock-in mouse model harboring one of the FEP mutations, Nav1.9 p.R222S [8,19].

Recently, a novel sodium channel blocker, ANP-230, was developed as a blocker of all three pain-related human subtypes, Nav1.7, Nav1.8, and Nav1.9. This drug is currently under Phase1/2 clinical trial in Japan as an oral therapeutic agent for the treatment of FEP syndrome.

Here, we have concurrently investigated the analgesic effects of ANP-230 on the behavioral and electrophysiological characteristics of the Nav1.9 p.R222S FEP model mice.

2. Material and Methods

2.1. Ethical statements

The maintenance and breeding of the mice employed in these studies followed the Animal Welfare Guidelines of Kyoto University, and the experimental protocols used were approved by the Animal Care, Use and Ethics Committee at Kyoto University (approval nos., Med Kyo 21054 and Med Kyo 22504; with approval dates, 23 Mar. 2021 and 15 Mar. 2022, respectively).

2.2. Animals

We used *Scn11a* p.R222S (R222S) knock-in heterozygous mice that we generated previously [10] together with C57BL/6 N WT (WT) mice (purchased from Japan SLC, Inc., Shizuoka, Japan) for the behavioral tests. Mice weighing 19–26 g were housed in plastic cages with ad libitum food and water under controlled temperature (24 ± 2 °C) and humidity (50 ± 10%) and a 14-h light/10-h dark cycle (lights on 07:00–21:00) prior to the start of experiments, and according to the Animal Welfare Guidelines of Kyoto University. Male mice, used at 6–8 weeks of age, were housed in cages with ad libitum food and water, and kept in a section of a refrigerator at 4 ± 2 °C for 14–15 h (overnight) before the behavioral experiments. All mice used in the these experiments were placed in the experimental room (20–23 °C) for 1 h for acclimatization and analyzed for their pain behavior before and after drug administration.

2.3. Administration of drugs

ANP-230 was kindly provided by AlphaNavi Pharma Inc. This patented drug (WO2010074193) was initially introduced as a Nav1.8 blocker [20], and is currently undergoing clinical trials (ISRCTN07951717, ISRCTN80154838). In this study, we investigated the effects of ANP-230 on the pain hypersensitivity of FEP model mice carrying the Nav1.9 R222S mutation.

For the behavioral tests, ANP-230 (3, 10, and 30 mg/kg, AlphaNavi Pharma Inc.) and pregabalin (10, 30 mg/kg, Sigma-Aldrich, St. Louis, MO, USA) as a control analgesic agent were each dissolved in 0.05% methylcellulose in PBS. These drugs or vehicle solutions (0.05% methylcellulose) were administered by oral injections. For electrophysiological studies, ANP-230 was further diluted with DMSO to yield a 30 mM solution, and then further diluted 1000-fold with extracellular solution. Two doses of ANP-230 (10 or 30 μM) were used for the dose-dependency studies.

2.4. Behavioral tests

Hot plate test: To detect the hyper-thermal response of the mice to noxious heat, we used a hot plate (NISSIN Co, NHP-45 N) with a pre-set plate temperature of 55 °C. The test mouse was placed onto the hot plate and the time taken (s) for it to respond, for example by licking, shaking or lifting of the hindpaws [21], was measured by the observer [22]. A cut-off time of 60 s was used to minimize the possibility of cutaneous tissue damage. We used 10 mg/kg pregabalin since a 30 mg/kg dose induced strong sedation beyond the

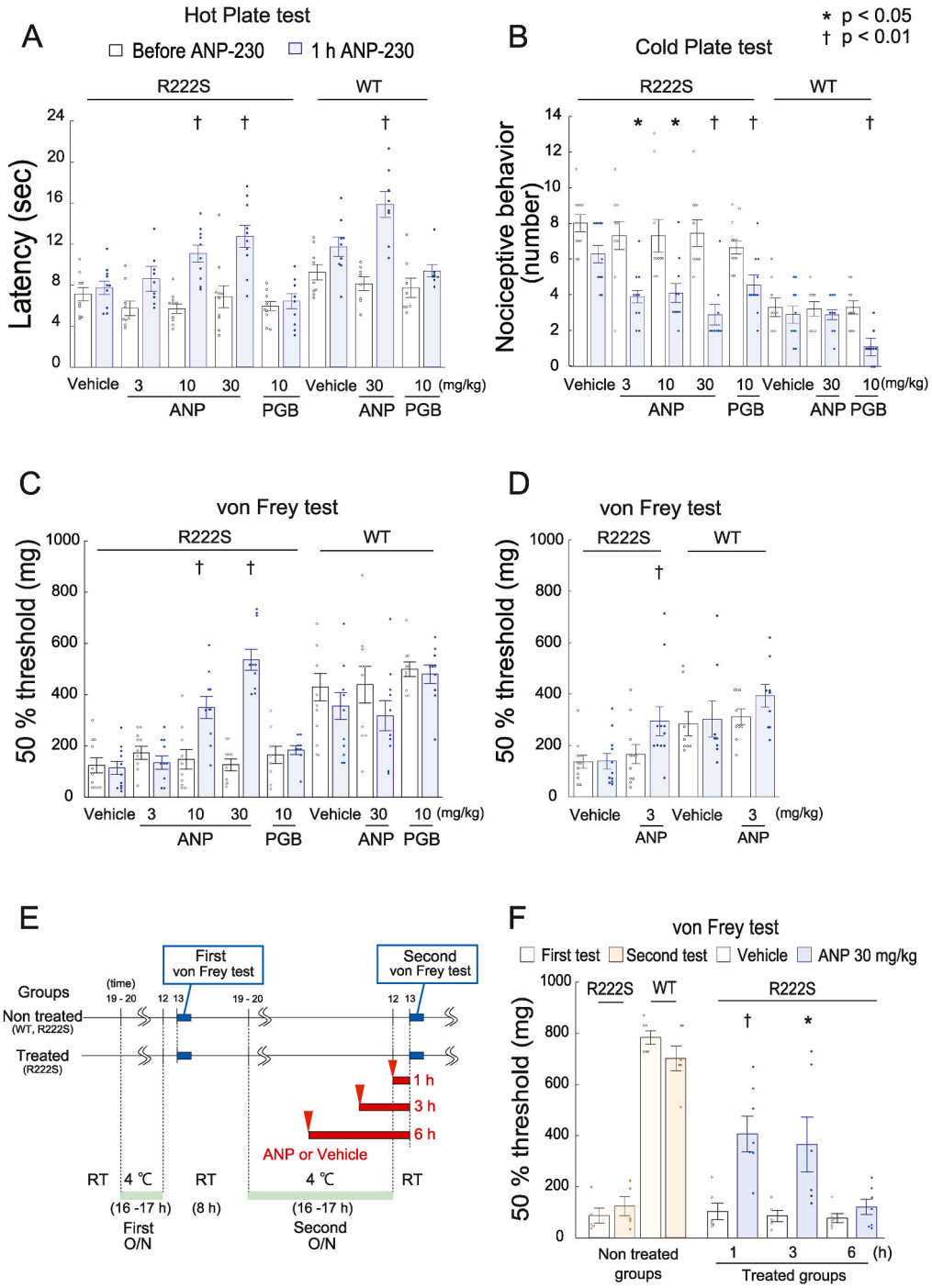

Fig. 1. The analgesic effects of ANP-230 on R222S mice. Reduced pain behavior by oral administration of ANP-230. (A) Dose-dependent inhibition of the hyper-thermal sensitivity of R222S and WT mice before and after 1 h ANP-230 (ANP) administration (R222S, n = 9–10; WT, n = 8–9). (B) Inhibition of the hypo-thermal sensitivity of R222S mice but not WT mice at each dose of ANP-230 (WT, n = 9–10; R222S, n = 9–11). Pregabalin (PGB) had an inhibitory effect on the hypo-thermal sensitivity of both mice groups but not on their hyper-thermal sensitivity. (C) Dose-dependent inhibition of the mechanosensitivity of R222S mice but not WT mice before and after ANP-230 administration (R222S, n = 9–11; WT, n = 10). (D) Reduction of the hyper-mechanosensitivity of R222S mice by repetitive administration of low dose (3 mg/kg) ANP-230 (R222S, n = 8–9; WT, n = 11). (E) Scheme showing the effects of the first and second cold periods on the mechanosensitivity of non treated WT and R222S groups, and of the time course administration of vehicle or ANP-230 on the mechanosensitivity of R222S mice. Two cold exposure periods were set to ensure complete cold exposure conditions. (F) Time course of ANP-230 (30 mg/kg) on the mechanosensitivity of R222S mice. No significant differences were observed between the first (beige) and second (orange) mechanosensitivity tests in R222S and WT mice (R222S, n = 5; WT, n = 6). The duration of the analgesic effects of ANP-230 on R222S mice (n = 5–7) continued for at least 3 h but not up to 6 h. In Figs. A to D, the white and blue bars

represent the before and after vehicle or drug administration, respectively (*p < 0.05, †p < 0.01 comparing before and after vehicle or drug administration; One way ANOVA), and in Fig. F the white and blue bars represent the vehicle or ANP-230 administration, respectively in the treated group (*p < 0.05, †p < 0.01 as compared to vehicle and drugs in treated group; two-sided Student's *t*-test). Data are presented as mean ± S.E.M. (For interpretation of the references to colour in this figure legend, the reader is referred to the Web version of this article.)

cut-off time.

Cold plate test: To detect the hypo-thermal sensitivity of the mice, each animal was placed individually in a transparent plastic cage (10 cm × 10 cm) and onto the cold plate (As one Co., SCP-85) with a floor temperature set to 10 °C. The total numbers of nociceptive behaviors (for example, lifting and shaking of paws and jumping) were counted for 3 min before and after drug administration.

Von Frey test: To detect the mechano-sensitivity of the mice, we performed the von Frey test using eight filaments with logarithmically incremental stiffness (0.02, 0.04, 0.07, 0.16, 0.4, 0.6, 1.0, and 1.4 g). Each mouse was placed on a stainless-steel mesh floor covered with a Plexiglas cage. The withdrawal response (biting, licking, lifting, or shaking) was evaluated at a 50% threshold, indicating the filament force at which an animal reacts in 50% of presentations [23].

We also investigated the analgesic effects of repeated administration of a low dose (3 mg/kg) of ANP-230, as well as a time course of the analgesic effects following administration of a high dose (30 mg/kg) of ANP-230. To detect the analgesic effects of repeated administration, mice were treated in the morning with either the vehicle or ANP-230 and then returned to their cages. These administrations were repeated over 6 consecutive days and then, at 6 days after the first treatment, the mechano-sensitivity of the mice were determined as described above.

To investigate the time course of the analgesic effects of ANP-230, two cold exposure [19] periods were set. After a first overnight cold exposure at 4 °C, the first von Frey tests were performed at room temperature and the mice were maintained under these conditions for a total of 8 h (Fig. 1E). The mice were then reexposed to a second over-night cold period, during which ANP-230 or vehicle was administered for 1, 3, or 6 h, and the mice then acclimatized to room temperature for 1 h before the second von Frey tests were performed (Fig. 1E). First, the sensitivity of the WT and R222S mice to the first and second cold treatments were compared (Fig. 1E). Subsequently, the effects of vehicle and ANP-230 on the sensitivity of the R222S mice during the second cold treatment period were compared (Fig. 1E). The cut off value was set for under 30 mg calculated for the filament force to a 50% threshold for each test.

2.5. Isolation of DRG neurons and electrophysiology

WT and R222S mice aged 6- to 8-weeks-old were used to isolate DRG neurons as described in our previous report [6]. Briefly, mice were anesthetized with sevoflurane, perfused transcardially with artificial cerebrospinal fluid (aCSF: 124 mM NaCl, 5 mM KCl, 1.2 mM KH_2PO_4, 1.3 mM $MgSO_4$, 2.4 mM $CaCl_2$, 10 mM glucose and 24 mM $NaHCO_3$), and the DRG neurons isolated from sections L4 to L6 of the spine. Incubation in collagenase XI (Sigma-Aldrich, St. Louis, MO, USA) diluted in Earle's balanced salt solution (Sigma-Aldrich, St. Louis, MO, USA) for 25 min at 37 °C was used to further isolate the DRG neurons, which were resuspended in aCSF and plated onto non-coated 12 mm φ coverslips.

Small diameter DRG neurons (<25 μm) were selected and used within 8 h after isolation for electrophysiological analysis at 23 – 25 °C. Patch pipettes were made from thin-walled borosilicate glass capillaries (GC150TF-10, Harvard Apparatus, MA, USA), pulled and fire-polished to a resistance of 4–6 MΩ prior to use. Electrode capacitance was electrically compensated with a series resistance of <13 MΩ. Cells were excluded from analysis if they required more than −30 pA to hold the membrane at −60 mV or if their series resistance changed by more than 25%.

Current clamp recordings were acquired after achieving more than 5 min of whole-cell recording conditions as in our previous study [8]. The pipette solution and the bath solution for isolated DRG neurons were the same as in our previous report [6]. To detect the effect of ANP-230, data were obtained before ANP-230 administration from cells in a stable state after at least 7 min. Drug effects were measured at least 3 min after drug administration, and washout data were also measured after perfused bath solution. For every cell, a series of 500 ms step current injections, from 10 to 260 pA in 25 pA increments, was applied to determine the current threshold and the firing frequency from the average AP number in each pulse. In every trial, RMP was measured at I = 0 prior to current injection. Current threshold was defined by the lowest input current injections, from 10 pA in 25 pA increments, which induced an AP in DRG neurons. The input impedance was measured as the voltage response amplitude at a current injection of 10 pA.

The following parameters of the first AP of the current threshold were measured: amplitude, maximum rate of rise/fall of AP, 100% AP width (measured at threshold), and threshold. Additionally, to detect the effect of ANP-230 on the continuous generation of APs, we measured the following parameters at current threshold; 1st amplitude of AHP was measured from the threshold to the end of the 1st AP. The curve of the depolarization after the 1st AP was fitted with the following equation: $f(x) = Y_0 + A \exp(-\text{invTau}^*x)$. Furthermore, the depolarized voltage level during the input currents (1st-amplitude of AHP) and AHP of the end of stimulus current were measured. We then calculated the means and SDs for vehicle and drug groups of WT and R222S mice. We excluded cells that either did not generate APs or had only one AP in response to a 500-ms current injection in all step pulses.

All data were obtained using Sutterpatch (Sutter Instrument). Electrophysiological data of these cells were analyzed using Igor Pro (WaveMetrics Inc., Portland, OR, USA).

2.6. Statistical analysis

All behavioral tests and electrophysiological data are presented as means ± standard error of the mean (S.E.M.). The behavioral

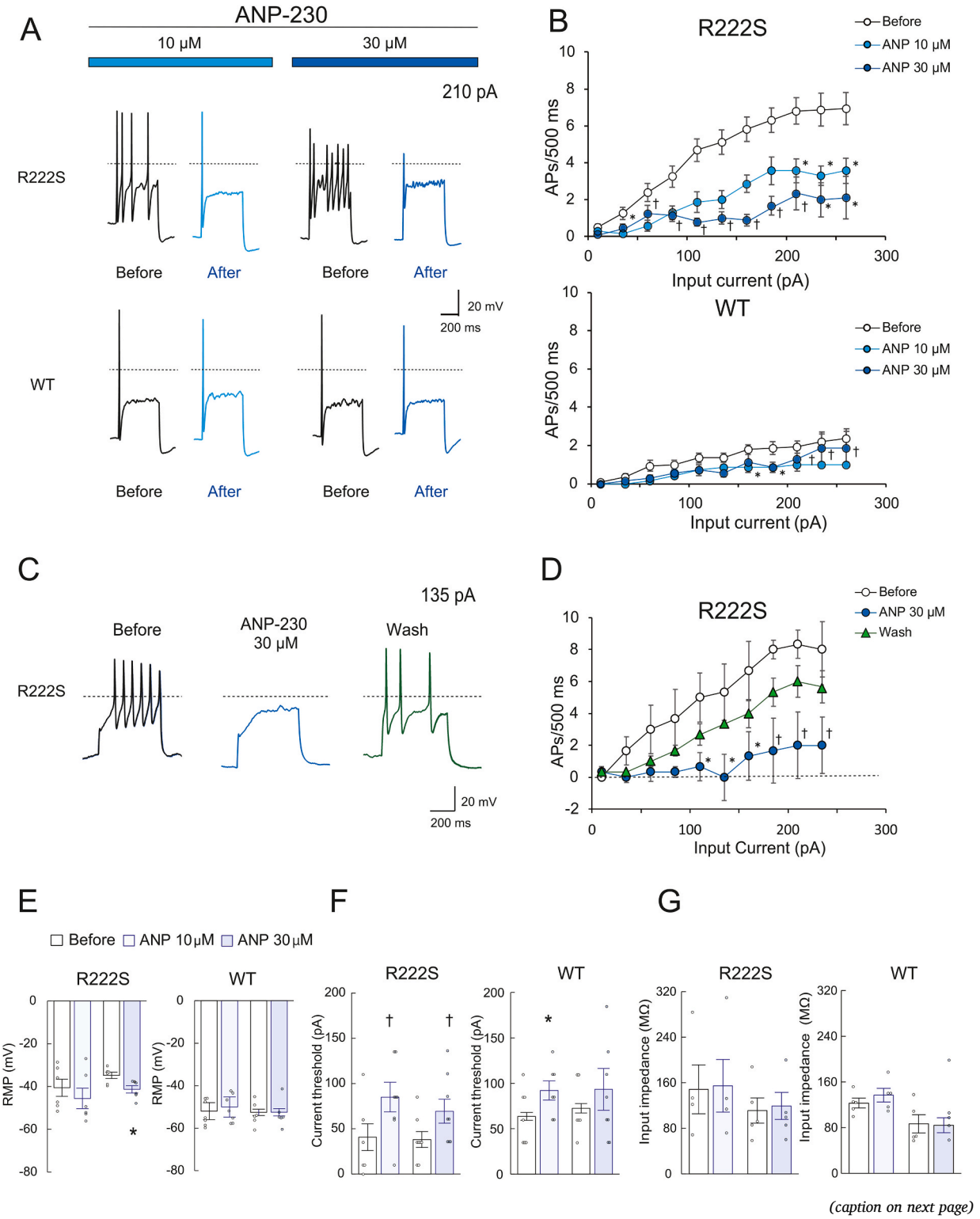

(caption on next page)

Fig. 2. ANP-230 reduces the hyperexcitability of small DRG of R222S mice. (A) Representative traces of the action potential (AP) firing before and after administration of 10 and 30 μM ANP-230, recorded from small DRG neurons (<25 μm) in R222S and WT at 210 pA during 500 ms. The decline of repetitive APs of R222S mice, but not in WT mice, by administration of ANP-230. Dashed lines represent the 0 mV in A and C. (B) Dose-dependent effects of ANP-230 on firing probability of DRG neurons of R222S (upper panel; Before, n = 16; ANP-230 10 μM, n = 7; ANP-230 30 μM, n = 9), but not in DRG neurons of WT (lower panel; Before, n = 14; ANP-230 10 μM, n = 7; ANP-230 30 μM, n = 7). The 500-ms-step current injections ranged from 10 to 210 pA. Data are presented as mean ± S.E.M. (*$p < 0.05$,†$p < 0.01$ in comparisons of before and after ANP-230 administration at each dose; two-sided Student's *t*-test). (C) The firing frequency partially reversed to hyperexcitable conditions by washout. Each trace is a representative trace recording at an input current of 135 pA before, after 30 μM ANP-230 administration, and after wash conditions. (D) The effect of ANP-230 on the firing frequency of R222S mice (n = 3) was significantly cleared by the wash conditions. (E) Shift in the resting membrane potential (RMP) of R222S and WT mice in response to ANP-230. The recovery of the polarized RMP towards hyperpolarization was significant in R222S mice (n = 6) at a high ANP-230 dose, but there was no shift in WT mice at either dose (n = 6–7). (F) Recovery of the depolarized current threshold of R222S mice by both doses of ANP-230 (R222S, n = 7–8; WT, n = 7–6). (G) Changes in input impedance in R222S and WT mice. There were no significant changes in input impedance following administration of ANP-230 at either dose (R222S, n = 4–5; WT, n = 5). Before ANP-230 administration is represented by black line traces, white dots and bars, and after 10 and 30 μM ANP-230 administration represented by blue and deep blue line traces, dots and bars, respectively. *$p < 0.05$, †$p < 0.01$ in comparisons of before and after administration or wash; two-sided Student's *t*-test. (For interpretation of the references to colour in this figure legend, the reader is referred to the Web version of this article.)

tests for the dose- and time dependent effects of ANP-230 administration and the firing frequencies were statistically compared between the vehicle and ANP-230 dose groups by two-sided Student's t-tests. All the AP parameter's statistical comparisons were based on a one-way ANOVA (comparisons between each ANP-230 dose and vehicle). Statistical significance is indicated by *, $p < 0.05$, and by †, $p < 0.01$.

3. Results

3.1. Behavioral tests

We first performed a hot plate test to validate the thermal withdrawal behavior of the mice, and used three different ANP-230 concentrations (3, 10, and 30 mg/kg) to evaluate the dose-dependent analgesic effects of the drug. The hyper-thermal sensitivity of the R222S mice was inhibited by oral administration of ANP-230 and this effect was clearly dose dependent (Fig. 1A). In addition, the hypo-thermal sensitivity of the R222S mice was examined by a cold plate test and found to be significantly attenuated even by the lowest ANP-230 dose (Fig. 1B). We also evaluated the effects of pregabalin on the thermal withdrawal behavior of the mice. Although 10 mg/kg pregabalin had no significant effect on the hyper-thermal sensitivity of either mouse genotype (Fig. 1A), it significantly reduced the hypo-thermal sensitivity of both WT and R222S mice (Fig. 1B).

We next evaluated the effect of ANP-230 on the mechanosensitivity of the mice using the von Frey test (Fig. 1C). ANP-230 reduced the hyper-mechanosensitivity of the R222S mice in a dose dependent manner and these effects were significant at both 10 and 30 mg/kg ANP-230. However, pregabalin showed no significant effects on either the WT or R222S mice. We also examined the effects of repetitive administration of low doses of ANP-230 on the mechanosensitivity of the mice, as the toxicological profile of ANP-230 following repeated administration is a critical safety test for clinical trials. Although administration of 3 mg/kg ANP-230 for 1 h prior to the von Frey test was not effective, repetitive administration of ANP-230 at this dose demonstrated significant analgesic effects on the R222S mice (Fig. 1D).

We subsequently investigated the duration that the analgesic effects of ANP-230 last after drug administration. ANP-230 was administered for 1, 3, or 6 h during a second overnight cold exposure period, which ensure full cold sensitivity in mice (Fig. 1E, see Material and Methods). To first evaluate the influence of the two cold exposure conditions, we compared the first overnight cold exposed condition with the second overnight cold exposure condition in the absence of any drug administration (non treated group). There were no significant differences between these two conditions in either the WT or R222S mice (Fig. 1F). We then investigated the time course of the analgesic effects of ANP-230 on the R222S mice (treated group), and found a significant inhibitory effect of ANP-230 on cold exposed pain after administration for 1 and 3 h when compared with the vehicle groups but not after 6 h of treatment (Fig. 1F).

These results confirm that ANP-230 can significantly reduce the hypersensitive pain responses of the R222S mice.

3.2. Electrophysiology

To examine the effects of ANP-230 on the hyperexcitability of DRG neurons, we performed electrophysiological experiments using perfusion of ANP-230 at two doses (10 μM or 30 μM) to DRG neurons isolated from WT and R222S mice. ANP-230 administration reduced the number of repetitive APs of the R222S-derived DRG neurons (Fig. 2A), in a dose dependent manner (Fig. 2B upper panel), with a dose of 30 μM ANP-230 reducing the number of APs to WT levels. In contrast to the effects of ANP-230 on R222S DRG neurons, its effects on WT DRG neurons was limited (Fig. 2B lower panel). Finally, the effects of ANP-230 on R222S DRG neurons were partially reversible by washout with control bathing solution (Fig. 2C and D), suggesting that ANP-230 may not have long-term toxicity effects.

The resting membrane potential (RMP) was significantly depolarized in DRG neurons of R222S in comparison with DRG neurons of WT (R222S: −37.69 ± 2.22 mV; WT: −52.25 ± 1.52 mV, $p < 0.01$), but became significantly polarized following administration of 30 μM ANP-230 (Before: −34.80 ± 1.48 mV; ANP-230: −41.32 ± 1.71 mV, $p < 0.05$, Fig. 2E). The current threshold of DRG neurons of R222S mice was also significantly increased by ANP-230 administration of 10 μM (Before: 40.71 ± 14.74 pA; ANP-230: 85.00 ± 16.37

pA, $p < 0.01$) and 30 μM (Before: 38.13 ± 8.76 pA; ANP-230: 69.38 ± 13.31 pA, $p < 0.01$, Fig. 2F). Although the RMP of DRG neurons of WT mice did not change in response to ANP-230 (Fig. 2E), there was a significant change in the current threshold of DRG neurons of WT mice following administration of 10 μM ANP-230 (Before: 63.57 ± 4.34 pA; ANP-230: 92.14 ± 10.51 pA, $p < 0.05$, Fig. 2F). Nevertheless, the input impedance did not change in either mouse strain following ANP-230 administration (Fig. 2G). These results indicate that the predominant effects of ANP-230 are to inhibit the burst firing of DRG neurons.

To detect the effects of ANP-230 on AP parameters, we calculated the following parameters from the 1st spike amplitudes generated near the current threshold (Table 1). In R222S mice, the amplitude and the maximum rate of rise were significantly reduced by administration of ANP-230 at each dose. However, only a high dose of ANP-230 at 30 μM significantly reduced the maximum rate of fall and width. The AP thresholds were not changed significantly by either dose of ANP-230. In WT mice, the spike amplitude was significantly reduced only by a high dose of ANP-230 at 30 μM, whereas the maximum rate of rise was significantly decelerated by each dose of ANP-230. However, the maximum rate of fall, width and threshold were not significantly affected in WT mice by ANP-230.

These results suggest that administration of ANP-230, especially at high doses, makes the AP less likely to overshoot, and that the shape of AP becomes smaller. On the other hand, in WT, the parameters that form the shape of the AP were not affected, and the amplitude of spikes and the rate of rise were finally affected at high concentrations.

To obtain insights into the pharmacological actions of ANP 230, we calculated several parameters for factors involved in continuous firing. As shown in Fig. 3A, we measured the magnitude of the after hyperpolarization (AHP) and the time constants of the AHP decay of the 1st spike. In R222S mice, the AHP of the 1st spike was significantly reduced by ANP-230 at the high dose of 30 μM (Before: 39.87 ± 6.65 mV; ANP-230: 31.18 ± 5.31 mV, $p < 0.05$, Fig. 3B). The magnitude of the time constant of the AHP decay of the 1st spike amplitude (tau) of R222S was slower than that of WT (R222S: 120.64 ± 19.03 ms, WT: 51.53 ± 4.60 ms, $p < 0.01$). In R222S, tau was significantly reduced by a high dose of ANP-230 at 30 μM (Before: 113.35 ± 28.08 ms; ANP-230: 56.69 ± 14.04 ms, $p < 0.01$, Fig. 3C). The change in voltage induced by current injection increased significantly in R222S after administration of ANP-230 at both 10 μM (Before: 16.15 ± 3.70 mV; ANP-230: 27.99 ± 5.35 mV, $p < 0.05$) and 30 μM (Before: 21.86 ± 3.83 mV; ANP-230: 33.32 ± 3.95 mV, $p < 0.01$, Fig. 3D), whereas the AHP of stimulus end was not significantly affected in R222S mice by ANP-230 (Fig. 3E). In WT mice, none of these parameters were affected by administration of ANP-230.

These results suggest that ANP-230 reduces the size of the overshoot of APs and thereby inhibits the hyperexcitability of DRG neurons of R222S mice.

4. Discussion

ANP-230 is a novel sodium channel blocker that has strong selectivity for Nav1.7, 1.8 and 1.9, and displays state- and use-independent Nav1.7 inhibition similar to guanidinium toxins, such as STX and TTX. ANP-230 has already completed several Phase 1 clinical studies in the US, UK and Japan, and is now undergoing a Phase 1/2 study in Japan for FEP patients predominantly carrying Nav1.9 mutations. Although verification of the inhibitory effects of ANP-230 on Nav1.9 mutations is complicated by difficulties in establishing a suitable cell-based expression system, some methods have already been described [24–26]. To overcome the inherent difficulties in such systems, we employed R222S mutant Nav1.9 mice, which display clear pain phenotypes, to investigate the analgesic effects of ANP-230 on FEP.

Here we show that the R222S hypersensitive pain behaviors could be significantly inhibited in a dose-dependent manner by administration of ANP-230, and that levels equivalent to WT could be recovered at higher doses of the drug (Fig. 1). The significant inhibition of the hyper-thermal sensitivity, but not of the hypo-thermal nor mechanical sensitivities, of the WT mice by high ANP-230 doses (Fig. 1A) may suggest that differential effects of ANP-230 on the hyper-thermal sensitivity may depend on the degree of Nav1.8 contribution to each mice. Pregabalin, a calcium channel inhibitor that is used as a clinically-prescribed analgesic, could inhibit the hypo-thermal pain sensitivity of both the R222S and WT mice, (Fig. 1B), but not the hyper-thermal nor mechanical sensitivity of the mice genotypes. Again, these differences in drug efficacy could be attributed to target channel differences. Furthermore, ANP-230 had a significant analgesic effect on R222S mice when administered repetitively at a low dose (Fig. 1D), and also for a duration of at least 3 h, but not up to 6 h, when administered at a high dose (Fig. 1E and F). The mechanism of this pain inhibition is unknown given that the

Table 1
Parameters of action potential at current threshold. *$p < 0.05$, †$p < 0.01$; two-sided Student's *t*-test.

					ANP-230				
Genotype	Parameter	n	Before	10 μM	p value	n	Before	30 μM	p value
R222S	Amplitude (pA)	7	88.66 ± 2.48	79.08 ± 4.44	<0.05	6	82.14 ± 7.55	68.56 ± 4.83	<0.05
	Maximum rate of rise time (mV/ms)	7	39.24 ± 4.33	28.65 ± 3.88	<0.05	6	49.51 ± 14.35	19.98 ± 7.24	<0.05
	Maximum rate of fall time (mV/ms)	7	−10.14 ± 2.16	−8.37 ± 2.40	n.s.	6	−17.42 ± 6.94	−10.99 ± 4.66	<0.05
	Width (ms)	7	7.25 ± 0.58	7.16 ± 0.74	n.s.	6	6.48 ± 1.28	7.45 ± 1.36	<0.05
	Threshold (mV)	7	−9.60 ± 0.79	−8.53 ± 1.74	n.s.	6	−9.78 ± 1.21	−11.28 ± 1.36	n.s.
WT	Amplitude (pA)	7	79.68 ± 10.55	68.17 ± 14.19	n.s.	5	83.01 ± 11.5	69.79 ± 12.26	<0.01
	Maximum rate of rise time (mV/ms)	8	34.87 ± 8.52	20.17 ± 5.14	<0.01	5	51.24 ± 5.53	27.08 ± 6.75	<0.01
	Maximum rate of fall time (mV/ms)	7	−15.87 ± 2.54	−13.13 ± 1.57	n.s.	4	−18.77 ± 2.27	−14.80 ± 2.76	n.s.
	Width (ms)	7	5.87 ± 0.84	6.04 ± 0.83	n.s.	5	5.12 ± 0.77	5.03 ± 0.61	n.s.
	Threshold (mV)	7	−8.50 ± 0.89	−7.66 ± 0.70	n.s.	4	−10.03 ± 0.71	−7.99 ± 0.86	n.s.

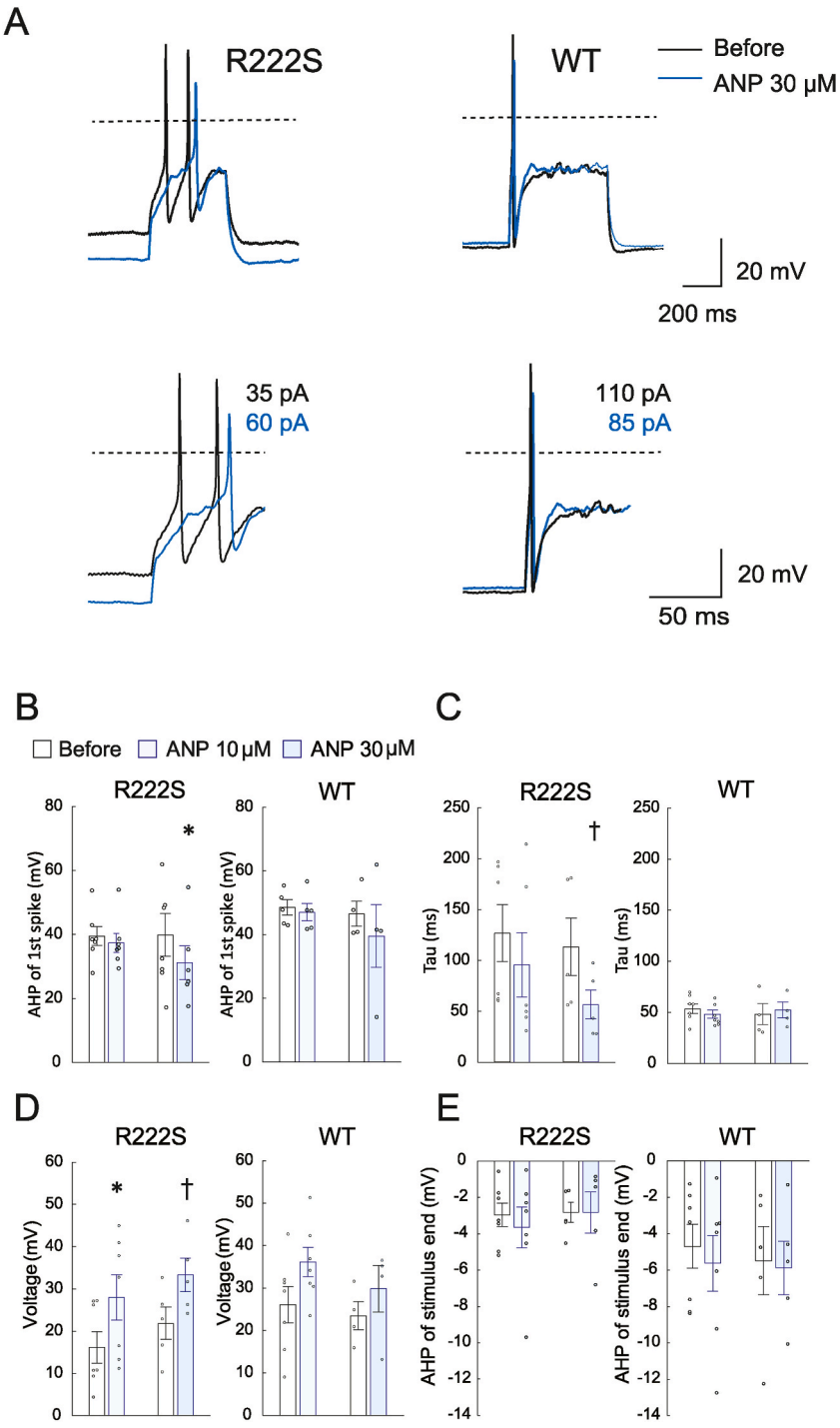

Fig. 3. Effects of ANP-230 on the accumulation of Na^+ currents in R222S mice. (A) Representative traces of AP firing before and after administration of ANP-230 at current threshold. The lower traces represent the expanded view of each 1st AP. Dashed lines represent the 0 mV. (B) The high ANP-230 dose significantly reduced the after hyperpolarization (AHP) of the 1st spike at current threshold in R222S mice (R222S, n = 6–7). (C) The high dose of ANP-230 significantly reduced the time constants of the AHP decay of the 1st spike (tau) in R222S mice (R222S, n = 5–6). (D) The recovery of depolarized voltage level during input currents at threshold current were significant at both ANP-230 doses in R222S (R222S, n = 5–7) but not in WT (WT, n = 4–7) mice. (E) No significant changes in the AHP of stimulus end to ANP-230 were observed in either R222S or WT mice. Color representations follow those in legend of Fig. 2. *$p < 0.05$, †$p < 0.01$ in comparisons of before and after administration or wash; two-sided Student's *t*-test. (For interpretation of the references to colour in this figure legend, the reader is referred to the Web version of this article.)

clearance of ANP-230 was transitory, and that the drug was neither toxic nor had any excessive sedative effects on WT mice. Therefore, these results may be representative of the clinical implications of ANP-230 on FEP.

In our current electrophysiological experiments we focused on the effects of ANP-230 on the Nav channels that are responsible for the repetitive APs in the R222S model mice. As shown in Fig. 2A and B, the continuous firing of R222S neurons was significantly interrupted by administration of ANP-230. These results may correlate with the inhibitory effect of ANP-230 on the increased current threshold (Fig. 2F), which is indicative of the maximum change of subthreshold by the input current necessary for AP firing. Nav1.9 could be involved in setting the RMP and enhancing the subthreshold depolarization in cooperation with Nav1.7 [4,27]. In R222S mice, the Nav1.9 mutation induced the depolarization of RMP compared with the WT. Therefore, these results indicate that the current threshold was determined by both Nav1.9 and Nav1.7, and that the inhibitory effect of ANP-230 was to influence the combined channels (Fig. 2E and F).

The parameters of maximum rate of rise and fall were significantly reduced, particularly after the application of a high ANP-230 dose (Table 1). It is well known that the maximum rate of rise and fall are indicative of the Nav1.7 and Nav1.8 currents in DRG neurons, with the Nav1.8 channel being the major contributor to the AP upstroke in small DRG neurons [4,28]. These results indicate therefore that ANP-230 inhibits the Nav1.7 and 1.8 channels in both mice genotypes.

We have also shown that the 1st spike amplitude-AHP, as well as the time constants of the AHP decay of the 1st spike amplitude (tau), were significantly reduced by the high ANP-230 dose (Fig. 3B and C). Furthermore, the increment of membrane potential during current input was increased by both ANP-230 doses, whereas the AHP at the stimulus end was not affected by either of the ANP-230 doses (Fig. 3D and E). The AHP of APs during repetitive firing was attributed to voltage- and calcium-dependent potassium channels [29], and the slowly decaying AHP during stimulation accumulated over time and lead to reduced excitability [30]. The AHP of the stimulus end was mediated by potassium channels, which largely contribute to AP repolarization [31–35]. These results may therefore suggest that inhibition of the Nav1.7, 1.8 and 1.9 channels prevents Na^+ influx but does not affect K^+ efflux, so that this effect influences the K^+-induced conductance changes during current injection, resulting in Na^+ accumulation and the subsequent suppression of firing.

Taken together, our results suggest that ANP-230 reduces the AP generated through the combined currents of the Nav1.9 mutation together with those of Nav1.7 and Nav1.8, and that inhibition of the membrane excitability of small DRG neurons by ANP-230 correlates well with the extent of inhibition of pain sensitivity of the R222S FEP model mice by ANP-230.

The current study has several limitations. First, the R222S mice are rodent models of FEP, and although the clinical phenotypes of FEP are well reproduced they are not complete [8]. Therefore, it is necessary to consider species differences, especially in the medicinal impact of ANP-230. Next, although we have demonstrated that ANP-230 reduces the frequency of AP generation and reduces the AP parameters, and that these are consistent with the suppression DRG neuron hyperexcitability, it is difficult to obtain pharmacological insights into the channel dynamics of Nav1.7–1.9, which constitute a composite AP. Therefore, the direct effects of ANP-230 on the Nav1.9 mutation channel properties by voltage clamp will need to be further investigated in subsequent studies.

In conclusion, we have demonstrated the inhibitory effects of ANP-230 on pain using FEP model mice harboring the Nav1.9 p.R222S mutation. We have also shown for the first time that ANP-230 suppresses the repetitive firing that is characteristic of this Nav1.9 mutation. These results indicate therefore that this drug may be useful as an effective analgesic agent that could replace the opioid drugs that are currently being used to treat various Nav 1.7–1.9 pain disorders.

Author contribution statement

Hiroko Okuda: Conceived and designed the experiments; Performed the experiments; Analyzed and interpreted the data; Contributed reagents, materials, analysis tools or data; Wrote the paper.

Sumiko Inoue: Performed the experiments; Wrote the paper.

Yoshihiro Oyamada: Conceived and designed the experiments; Analyzed and interpreted the data; Contributed reagents, materials, analysis tools or data; Wrote the paper.

Akio Koizumi; Shohab Youssefian: Conceived and designed the experiments; Analyzed and interpreted the data; Wrote the paper.

Data availability statement

Data included in article/supp. material/referenced in article.

Additional information

No additional information is available for this paper.

Declaration of interest's statement

The authors declare that they have no known competing financial interests or personal relationships that could have appeared to influence the work reported in this paper.

Acknowledgments

We thank Drs. Harunori Ohmori and Kouji H Harada for valuable discussions, technical support, and statistical analysis of the data, and also Zhaoqing Lyu and Li Meng for technical assistance.

References

[1] D.L. Bennett, X.A.J. Clark, J. Huang, S.G. Waxman, S.D. Dib-Hajj, The role of voltage-gated sodium channels in pain signaling, Physiol. Rev. 99 (2) (2019) 1079–1151, https://doi.org/10.1152/physrev.00052.2017.
[2] M. Costigan, J. Scholz, C.J. Woolf, Neuropathic pain: a maladaptive response of the nervous system to damage, Annu. Rev. Neurosci. 32 (2009) 1–32, https://doi.org/10.1146/annurev.neuro.051508.135531.
[3] T.R. Cummins, S.D. Dib-Hajj, S.G. Waxman, Electrophysiological properties of mutant Nav1.7 sodium channels in a painful inherited neuropathy, J. Neurosci. 24 (2004) 8232–8236, https://doi.org/10.1523/JNEUROSCI.2695-04.
[4] S.D. Dib-Hajj, T.R. Cummins, J.A. Black, S.G. Waxman, Sodium channels in normal and pathological pain, Annu. Rev. Neurosci. 33 (2010) 325–347, https://doi.org/10.1146/annurev-neuro-060909-153234.
[5] M.D. Baker, M.A. Nassar, Painful and painless mutations of SCN9A and SCN11A voltage-gated, P Flugers Arch. 472 (7) (2020) 865–880, https://doi.org/10.1007/s00424-020-02419-9.
[6] X.Y. Zhang, J. Wen, W. Yang, C. Wang, L. Gao, L.H. Zheng, et al., Gain-of-function mutations in SCN11A cause familial episodic pain, Am. J. Hum. Genet. 93 (5) (2013) 957–966, https://doi.org/10.1016/j.ajhg.2013.09.016. PMID: 24207120.
[7] E. Leipold, A. Hanson-Kahn, M. Frick, P. Gong, J.A. Bernstein, et al., Cold-aggravated pain in humans caused by a hyperactive NaV1.9 channel mutant, Nat. Commun. 6 (2015), 10049, https://doi.org/10.1038/ncomms10049. PMID: 26645915.
[8] H. Okuda, A. Noguchi, H. Kobayashi, D. Kondo, K.H. Harada, et al., Infantile pain episodes associated with novel Nav1.9 mutations in familial episodic pain syndrome in Japanese families, PLoS One 11 (5) (2016), e0154827, https://doi.org/10.1371/journal.pone.0154827. PMID: 27224030.
[9] C. Han, Y. Yang, R.H.T. Morsche, J.P. Drenth, J.M. Politei, et al., Familial gain-of-function Nav1.9 mutation in a painful channelopathy, J. Neurol. Neurosurg. Psychiatry 88 (3) (2017) 233–240, https://doi.org/10.1136/jnnp-2016-313804. PMID: 27503742.
[10] E. Leipold, L. Liebmann, G.C. Korenke, T. Heinrich, S. Giesselmann, et al., A de novo gain-of-function mutation in SCN11A causes loss of pain perception, Nat. Genet. 45 (11) (2013) 1399–1404, https://doi.org/10.1038/ng.2767. PMID: 24036948.
[11] C.G. Woods, M.O. Babiker, I. Horrocks, J. Tolmie, I. Kurth, The phenotype of congenital insensitivity to pain due to the NaV1.9 variant p.L811P, Eur. J. Hum. Genet. 23 (5) (2015) 561–563, https://doi.org/10.1038/ejhg.2014.166. PMID: 25118027.
[12] V. Phatarakijnirund, S. Mumm, W.H. McAlister, D.V. Novack, D. Wenkert, et al., Congenital insensitivity to pain: fracturing without apparent skeletal pathobiology caused by an autosomal dominant, second mutation in SCN11A encoding voltage-gated sodium channel 1.9, Bone 84 (2016) 289–298, https://doi.org/10.1016/j.bone.2015.11.022. PMID: 26746779.
[13] M.K. King, E. Leipold, J.M. Goehringer, I. Kurth, T.D. Challman, Pain insensitivity: distal S6-segment mutations in NaV1.9 emerge as critical hotspot, Neurogenetics 18 (3) (2017) 179–181, https://doi.org/10.1007/s10048-017-0513-9. PMID: 28289907.
[14] J. Huang, C. Han, M. Estacion, D. Vasylyev, J.G. Hoeijmakers, et al., Gain-of-function mutations in sodium channel Na(v)1.9 in painful neuropathy, Brain 137 (Pt 6) (2014) 1627–1642, https://doi.org/10.1093/brain/awu079. PMID: 2477697.
[15] C. Han, Y. Yang, B.T. de Greef, J.G. Hoeijmakers, M.M. Gerrits, et al., The domain II S4-S5 linker in Nav1.9: a missense mutation enhances activation, impairs fast inactivation, and produces human painful neuropathy, NeuroMolecular Med. 17 (2) (2015) 158–169, https://doi.org/10.1007/s12017-015-8347-9. PMID: 25791876.
[16] I.P. Kleggetveit, R. Schmidt, B. Namer, H. Salter, T. Helås, et al., Pathological nociceptors in two patients with erythromelalgia-like symptoms and rare genetic Nav 1.9 variants, Brain Behav. 6 (10) (2016), e00528, https://doi.org/10.1002/brb3.528. PMID: 27781142.
[17] J. Huang, Y. Yang, P. Zhao, M.M. Gerrits, J.G. Hoeijmakers, et al., Small-fiber neuropathy Nav1.8 mutation shifts activation to hyperpolarized potentials and increases excitability of dorsal root ganglion neurons, J. Neurosci. 33 (2013) 14087–14097, https://doi.org/10.1523/JNEUROSCI.2710-13.
[18] R. Kabata, H. Okuda, A. Noguchi, D. Kondo, M. Fujiwara, et al., Familial episodic limb pain in kindreds with novel Nav1.9 mutations, PLoS One 13 (2018), e0208516, https://doi.org/10.1371/journal.pone.0208516.
[19] Y. Matsubara, H. Okuda, K.H. Harada, S. Youssefian, A. Koizumi, Mechanical allodynia triggered by cold exposure in mice with the Scn11a p.R222S mutation: a novel model of drug therapy for neuropathic pain related to Na V 1.9, Naunyn Schmiedebergs Arch. Pharmacol. 394 (2) (2021) 299–306, https://doi.org/10.1007/s00210-020-01978-z.
[20] T. Gareth, D.J. Posson, Peter A. Goldstein, Voltage-gated ion channels in the PNS: novel therapies for neuropathic pain? Trends Pharmacol Sci. 37 (7) (2016) 522–542, https://doi.org/10.1016/j.tips.2016.05.002.
[21] A.W. Bannon, A.B. Malmberg, Models of nociception: hot-plate, tail-flick, and formalin tests in rodents, Curr. Protoc. Neurosci. (2007), https://doi.org/10.1002/0471142301.ns0809s41. Chapter 8: Unit 8.9.
[22] S. Hestehave, G. Munro, R. Christensen, T.B. Pedersen, L. Arvastson, et al., Is there a reasonable excuse for not providing post-operative analgesia when using animal models of peripheral neuropathic pain for research purposes? PLoS One 12 (11) (2017), e0188113 https://doi.org/10.1371/journal.pone.0188113.
[23] S.R. Chaplan, F.W. Bach, J.W. Pogrel, J.M. Chung, T.L. Yaksh, Quantitative assessment of tactile allodynia in the rat paw, J. Neurosci. Methods 53 (1994) 55–63, https://doi.org/10.1016/0165-0270(94)90144-9.
[24] Z. Lin, S. Santos, K. Padilla, D. Printzenhoff, N.A. Castle, Biophysical and pharmacological characterization of Nav1.9 voltage dependent sodium channels stably expressed in HEK-293 cells, PLoS One 11 (8) (2016), https://doi.org/10.1371/journal.pone.0161450.
[25] X. Zhou, Z. Xiao, Y. Xu, Y. Zhang, D. Tang, et al., Electrophysiological and pharmacological analyses of Nav1.9 voltage-gated sodium channel by establishing a heterologous expression system, Front. Pharmacol. 8 (NOV) (2017) 1–12, https://doi.org/10.3389/fphar.2017.00852.
[26] D.V. Sizova, J. Huang, E.J. Akin, M. Estacion, C.G. Perez, et al., A 49-residue sequence motif in the C terminus of Nav1.9 regulates trafficking of the channel to the plasma membrane, J. Biol. Chem. 295 (4) (2020) 1077–1090, https://doi.org/10.1016/s0021-9258(17)49917-0.
[27] T.R. Cummins, S.D. Dib-Hajj, J.A. Black, A.N. Akopian, J.N. Wood, et al., A novel persistent tetrodotoxin-resistant sodium current in SNS-null and wild-type small primary sensory neurons, J. Neurosci. 20 (22) (2000) 8493–8503, https://doi.org/10.1523/JNEUROSCI.20-22-08493.2000.
[28] A.M. Rush, T.R. Cummins, S.G. Waxman, Multiple sodium channels and their roles in electrogenesis within dorsal root ganglion neurons, J Physiol. 579 (Pt 1) (2007) 1–14, https://doi.org/10.1113/jphysiol.2006.121483.
[29] B.D. Bennett, J.C. Callaway, C.J. Wilson, Intrinsic membrane properties underlying spontaneous tonic firing in neostriatal cholinergic interneurons, J Neurosci. 20 (22) (2000) 8493–8503, https://doi.org/10.1523/JNEUROSCI.20-22-08493.2000.
[30] K.J. Hildebrandt, J. Benda, R.M. Hennig, The origin of adaptation in the auditory pathway of locusts is specific to cell type and function, J Neurosci. 29 (8) (2009) 2626–2636, https://doi.org/10.1523/JNEUROSCI.4800-08.
[31] A.A. Grace, B.S. Bunney, Intracellular and extracellular electrophysiology of nigral dopaminergic neurons: II. Action potential generating mechanisms and morphological correlates, Neuroscience 10 (1983) 317–331, https://doi.org/10.1016/0306-4522(83)90136-7.
[32] A.A. Grace, B.S. Bunney, The control of firing pattern in nigral dopamine neurons: single spike firing, J. Neurosci. 4 (1984) 2866–2876, https://doi.org/10.1523/JNEUROSCI.04-11-02866.1984.

[33] Y. Matsuda, K. Fujimura, S. Yoshida, Two types of neurons in the substantia nigra pars compacta studied in a slice preparation, Neurosci. Res. 5 (1987) 172–179, https://doi.org/10.1016/0168-0102(87)90033-2.
[34] T. Kita, H. Kita, S.T. Kitai, Electrical membrane properties of rat substantia nigra compacta neurons in an in vitro slice preparation, Brain Res. 372 (1986) 21–30, https://doi.org/10.1016/0006-8993(86)91454-x.
[35] C. J Wilson, J.A. Goldberg, Origin of the slow after hyperpolarization and slow rhythmic bursting in striatal cholinergic interneurons, J Neurophysiol. 95 (1) (2006) 196–204, https://doi.org/10.1152/jn.00630.2005.